REFERENCES

1. A. Eucken, Warmeleitfahigkeit Keramischer feuerfester stoffe; Berechnung aus der Warmeleitfahigkeit der Berstandeile, *Forsch. Geb. IngWes.* B3 **353**, 16 (1932).
2. I. I. Sherif, The relationship between bulk density and thermal conductivity in refractory insulating bricks, *Silicates Industriels* **28**(7–8), 1–2 (1963).
3. R. G. Diessler and G. S. Boegil, An investigation of effective thermal conductivity of powders in various gases, *Trans. Am. Soc. Mech. Engrs* **80**, 1417 (1958).
4. S. C. Cheng and R. I. Vachon, The prediction of the thermal conductivity of two and three phase solid heterogeneous mixtures, *Int. J. Heat Mass Transfer* **12**, 249–264 (1969).
5. G. Haacke and D. P. Spitzer, Method for thermal conductivity measurements on solids, *J. Scient. Instrum.* **42**, 702–704 (1965).

Int. J. Heat Mass Transfer. Vol. 19, pp. 229–231. Pergamon Press 1976. Printed in Great Britain

ANALYSIS OF MIXED CONVECTION ABOUT A HORIZONTAL CYLINDER

E. M. SPARROW and L. LEE
Department of Mechanical Engineering, University of Minnesota, Minneapolis, MN 55455, U.S.A.

(*Received* 18 *February* 1975 *and in revised form* 7 *April* 1975)

NOMENCLATURE

D,	cylinder diameter;
Gr_D,	Grashof number, $g\beta(T_w - T_\infty)D^3/\nu^2$;
g,	acceleration of gravity;
h,	local heat-transfer coefficient;
k,	thermal conductivity;
Nu,	Nusselt number, hR/k;
Nu_0,	hR/k at stagnation point;
Nu_x,	Nusselt number, hx/k;
Pr,	Prandtl number;
q,	local heat flux;
R,	cylinder radius;
Re_D,	Reynolds number, $U_\infty D/\nu$;
Re_x,	Reynolds number, Ux/ν;
T_w,	wall temperature;
T_∞,	free stream temperature;
U,	local free stream velocity;
U_∞,	velocity of approach flow;
u_i,	coefficients, equation (1);
X,	dimensionless coordinate, x/L;
x, y,	coordinates.

Greek symbols

β,	thermal expansion coefficient;
ν,	kinematic viscosity;
ϕ,	angular coordinate;
Ω,	mixed convection parameter, equations (6) and (7).

INTRODUCTION

HEAT transfer from horizontal cylinders under conditions of combined forced and natural convection flow has been the subject of numerous experimental studies, and [1–7] are representative of the available literature. On the other hand, aside from correlation efforts, there appears to have been little analytical study of the problem. Although the general case of mixed convection about a heated horizontal cylinder situated in an arbitrarily oriented forced convection flow is not readily amenable to analysis, it is possible to obtain solutions for a less general version of the problem. As will be demonstrated here, the case of an isothermal heated cylinder in a vertical forced convection upflow can be solved provided that a boundary-layer region exists. This fact was recognized by Acrivos [8], who obtained the $Pr \to 0$ and $Pr \to \infty$ limits for the Nusselt number at the lower stagnation point.

It is well established that for both forced convection and natural convection, a boundary-layer flow will exist on the lower part of the cylinder for moderate and large values of the Reynolds and Grashof numbers. Such a boundary-layer flow should also exist for mixed convection under aiding conditions.

For the isothermal cylinder, the separate forced convection and natural convection boundary layers possess an interesting common characteristic, namely, that they both have the same dependence on the streamwise coordinate (measured from the lower stagnation point). Consequently, the corresponding mixed convection problem retains this same streamwise dependence. Therefore, the mixing of the two forms of convection is not, in itself, the cause of boundary-layer nonsimilarity. This outcome is in contrast to mixed convection problems for other geometries such as horizontal plates and vertical plates and cylinders, where the mixing of the two flows causes nonsimilarity.*

ANALYSIS

A schematic diagram of the horizontal cylinder problem showing coordinates and nomenclature is given in Fig. 1. The boundary-layer flow is driven both by the external pressure gradient dp/dx due to the free stream velocity of the forced convection and by the buoyancy force $g\beta\rho(T - T_\infty)\sin\phi$. Via Bernoulli's equation, the pressure gradient is replaced by $-\rho U(dU/dx)$, where U is the local free stream velocity which, for a cylinder, can be represented by

$$U = u_1(x/R) + u_3(x/R)^3 + u_5(x/R)^5 + \ldots \quad (1)$$

The constants $u_1, u_3, u_5, \ldots$ differ from those for potential flow due to displacement of the streamlines which results from boundary-layer separation. Values measured by several investigators are given in [9]. For the buoyancy term, the expansion of the $\sin\phi$ factor, with $\phi = x/R$, is

$$\sin\phi = (x/R) - (1/6)(x/R)^3 + (1/120)(x/R)^5 + \ldots \quad (2)$$

Inspection of equations (1) and (2) suggests the similarity of the x-dependence of the two force components which drive the boundary-layer flow, and this may be confirmed by a complete evaluation of the respective terms.

The first term of the respective series (1) and (2) pertains to the lower stagnation point. If the conventional constant property momentum equation and non-dissipative energy equation are used, with the aforementioned pressure and buoyancy forces as inputs to the former, and a similarity

*In those cases, similarity may be achieved if contrived boundary conditions are employed.

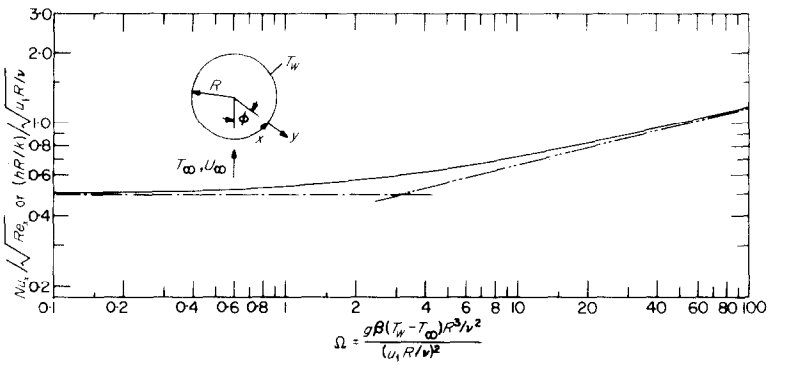

FIG. 1. Stagnation point heat transfer results, $Pr = 0{\cdot}7$.

transformation is carried out, there results for the stagnation point

$$f_1''' + f_1 f_1'' - f_1'^2 + \Omega\theta_0 + 1 = 0 \quad (3)$$

$$\theta_0'' + Prf_1\theta_0' = 0 \quad (4)$$

with boundary conditions

$$f_1(0) = f_1'(0) = \theta_0(\infty) = 0,\ \theta_0(0) = f_1'(\infty) = 1. \quad (5)$$

In addition to the Prandtl number Pr, these equations contain another parameter Ω whose definition is

$$\Omega = \frac{g\beta(T_w - T_\infty)R^3/\nu^2}{(u_1 R/\nu)^2}. \quad (6)$$

The numerator and denominator respectively represent a Grashof number and the square of a Reynolds number. Inasmuch as $u_1 = CU_\infty$, where $C \sim 1{\cdot}8$, Ω can be rephrased as

$$\Omega = \frac{g\beta\Delta TD^3/\nu^2}{(U_\infty D/\nu)^2}\frac{1}{2C^2} = \frac{Gr_D/Re_D^2}{2C^2} \cong 0{\cdot}15\frac{Gr_D}{Re_D^2}. \quad (7)$$

The transformation that led to equations (3)–(5) was patterned after that for pure forced convection, i.e.

$$\eta = y\sqrt{(u_1/\nu R)},\quad \psi = (\nu u_1 x^2/R)^{\frac{1}{2}} f_1(\eta) \quad (8a)$$

$$\theta_0(\eta) = (T - T_\infty)/(T_w - T_\infty). \quad (8b)$$

Alternatively, a transformation patterned after that for pure natural convection might have been employed, yielding a set of governing equations different from (3)–(5). During the course of the numerical computations, which spanned the range from $\Omega = 0$ to $\Omega = \infty$, it was found convenient to employ equations (3)–(5) for small and intermediate Ω, and to use the alternate set of equations for intermediate and large Ω. It was verified that the two sets of equations gave the same results.

For the solution away from the stagnation region, a Blasius series was employed on the basis of its satisfactory performance in the pure forced convection and pure natural convection problems [10–13]. The momentum and energy equations were reduced to ordinary differential equations by the series

$$\psi = (\nu R/u_1)^{\frac{1}{2}}(u_1 Xf_1(\eta) + 4u_3 X^3 f_3(\eta) + 6u_5 X^5 f_5(\eta) + \ldots) \quad (9)$$

$$\theta = \theta_0(\eta) + X^2\theta_2(\eta) + X^4\theta_4(\eta) + \ldots \quad (10)$$

in which $X = x/R$ and θ now represents $(T - T_\infty)/(T_w - T_\infty)$.

The differential equations for the f_i and θ_k were found to contain $u_1, u_3, u_5, \ldots$ as parameters. To eliminate the parameters, universal functions were deduced. Owing to the mutual coupling between the f and θ equations, the task of determining the universal functions was more demanding than that for cases where the velocity is independent of the temperature. The final slate of universal functions is

$$f_3 = f_{31} + (u_1/u_3)f_{32},\quad \theta_2 = (u_3/u_1)\theta_{21} + \theta_{22} \quad (11)$$

$$f_5 = f_{51} + (u_3^2/u_1 u_5)f_{52} + (u_3/u_5)f_{53} + (u_1/u_5)f_{54} \quad (12a)$$

$$\theta_4 = (u_5/u_1)\theta_{41} + (u_3/u_1)^2\theta_{42} + (u_3/u_1)\theta_{43} + \theta_{44}. \quad (12b)$$

The subscript notation was selected to indicate the mutual coupling of the functions. Thus, for example, f_{31} and θ_{21} are a coupled pair, as are f_{51} and θ_{41}, etc. With the subdivision of the functions indicated by equations (11) and (12), the differential equations and boundary conditions for the f_{ij} and θ_{kj} are readily derived. They will be omitted here to conserve space.

Numerical solutions were carried out using Gill–Runge–Kutta integration in conjunction with a shooting method to fulfil the boundary conditions at large η.

RESULTS

For the solutions, the Prandtl number was fixed at 0·7 (gases). The range of the mixed convection parameter Ω extended from zero to infinity and was covered by about 25 values. Local heat-transfer results were deduced from the solutions via Fourier's law. If $h = q/(T_w - T_\infty)$, then

$$(hR/k)/\sqrt{(u_1 R/\nu)} = -(\theta_0'(0) + (x/R)^2\theta_2'(0) + (x/R)^4\theta_4'(0) + \ldots). \quad (13)$$

The derivatives appearing in equation (13) were evaluated in terms of the universal functions of equations (11) and (12b).

At the stagnation point, where $U = u_1(x/R)$, equation (13) reduces to

$$(hR/k)/\sqrt{(u_1 R/\nu)} = (hx/k)/\sqrt{(Ux/\nu)} = Nu_x/\sqrt{Re_x} = -\theta_0'(0). \quad (14)$$

The stagnation point heat-transfer results evaluated from equation (14) are plotted in Fig. 1 as a function of the mixed convection parameter. Also appearing in the figure are two dashed lines which represent the pure forced convection and pure natural convection asymptotes. The equations of these lines are

$$Nu_x/\sqrt{Re_x} = 0{\cdot}4959,\quad Nu_x/\sqrt{Re_x} = 0{\cdot}3702\Omega^{\frac{1}{4}}. \quad (15)$$

The maximum deviation between the true solution and the envelope formed by the asymptote lines occurs at $\Omega \sim 3{\cdot}2$ and is about 20 per cent. As expected, under aiding conditions, the transfer coefficients for mixed convection exceed those for either pure forced convection or pure natural convection.

The asymptote lines facilitate determination of the conditions for which mixed convection prevails at the stagnation point. If the onset of mixed convection is defined in terms of five per cent deviations from the pure flows, the mixed convection range is $0{\cdot}6 < \Omega < 26$.

An abbreviated listing of the $\theta_0'(0)$ values used to construct Fig. 1 is given in Table 1. The lower half of the table contains values of $[\theta_0'(0)]/\Omega^{\frac{1}{4}}$ in deference to the approach to pure natural convection at large Ω.

To facilitate the evaluation of local heat-transfer coefficients at locations $\phi = x/R$ away from the stagnation point, a listing of derivatives $\theta_{kj}'(0)$ is given in Table 2. For the larger Ω, values of $(\theta_{kj}'(0))/\Omega^{\frac{1}{4}}$ are tabulated to show the

Table 1. Stagnation point results

Ω	0	0·2	0·5	1	2	4	6
$-\theta_0'(0)$	0·4959	0·5051	0·5179	0·5370	0·5694	0·6200	0·6598
Ω		10	20	60	160	400	∞
$(-\theta_0'(0))/\Omega^{\frac{1}{2}}$		0·4059	0·3919	0·3802	0·3754	0·3731	0·3702

Table 2. Values of $\theta_{kj}'(0)$ for $0 \leqslant \Omega \leqslant 6$ and $(\theta_{kj}'(0))/\Omega^{\frac{1}{2}}$ for $10 \leqslant \Omega \leqslant \infty$

Ω	$kj = 21$	22	41	42	43	44
0	−0·4476	0	−0·5860	0·1906	0	0
0·2	−0·4175	0·00179	−0·5432	0·1304	−0·00403	−0·000161
0·5	−0·3805	0·00406	−0·4912	0·06942	−0·00785	−0·000335
1	−0·3340	0·00704	−0·4265	0·01096	−0·01106	−0·000516
2	−0·2727	0·01130	−0·3426	−0·03809	−0·01287	−0·000693
4	−0·2060	0·01662	−0·2533	−0·06065	−0·01220	−0·000807
6	−0·1692	0·02008	−0·2050	−0·06156	−0·01086	−0·000837
10	−0·07229	0·01389	−0·08586	−0·03079	−0·00493	−0·000475
20	−0·04050	0·01485	−0·04668	−0·01907	−0·00256	−0·000393
160	−0·00660	0·01589	−0·00678	−0·00301	−0·000372	−0·000247
∞	0	0·01609	0	0	0	−0·000186

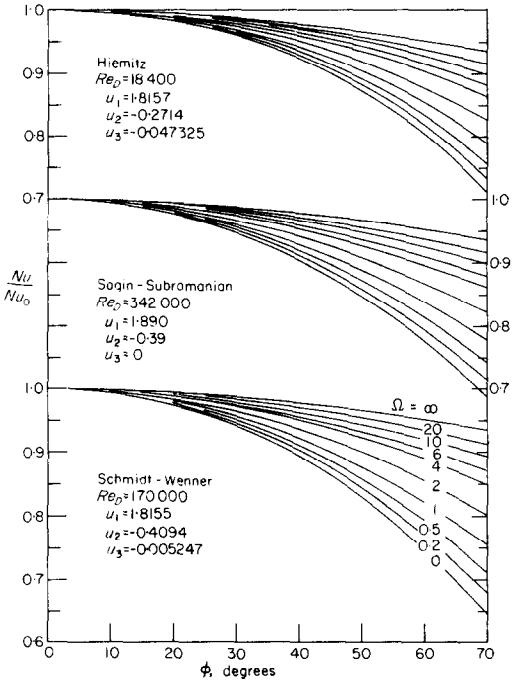

FIG. 2. Illustrative angular distributions of the local heat-transfer coefficient, $Pr = 0{\cdot}7$.

approach to the natural convection limit. Table 2 is used in conjunction with equations (13), (11), and (12b). Values of $\theta_{kj}'(0)$ at other Ω are available on request, but those of Table 2 should be sufficient. The results of Tables 1 and 2 for the limiting cases of $\Omega = 0$ and $\Omega = \infty$ agree very well with those in the literature, with the exception of $\theta_{44}'(0)$. In that case, the prior investigations [12, 13] do not agree among themselves, and it is felt that the present value is correct owing to superior computing equipment now available.

In order to obtain heat-transfer coefficients from equation (13), numerical values are needed for the coefficients $u_1, u_3, u_5, \ldots$ in the representation of the free stream velocity (equation (1)). It does not appear that any experimental information for the free stream velocity distribution in mixed convection is presently available. Therefore, at present, definitive results for the angular distribution of the heat-transfer coefficient cannot be obtained. It is, however, still worthwhile to illustrate the results using whatever information is available, and this has been done in Fig. 2.

In the figure, the local Nusselt number $Nu = hR/k$ at an angular position ϕ is plotted relative to the corresponding stagnation point value Nu_0. The angular coordinate that appears on the abscissa was terminated at 70° owing to the expected boundary layer separation. Three sets of results are given, corresponding respectively to the free stream velocity measurements of Hiemitz, Sogin and Subramanian, and Schmidt and Wenner (see [9]). The main message of the figure is that there is a substantially greater angular dependence when forced convection is dominant (small Ω) than when natural convection is dominant (large Ω).

It is relevant to consider comparisons between the present results and those of experiment. Such comparisons are difficult to make because the analysis provides local results for a portion of the cylinder whereas the experimental results are in the form of average coefficients for the entire cylinder. Furthermore, many of the experiments were performed at Reynolds and Grashof numbers that are below the values needed to ensure the existence of a boundary layer and, in other cases, fluids other than gases were employed.

The experiments of [4] appear to be the most appropriate candidate for comparison with the analytical results. In [4], the average Nusselt number for mixed convection is compared with that for pure forced convection, the ratio being correlated as a function of Gr_D/Re_D^2 in the range of this parameter from zero to nine. At $Gr_D/Re_D^2 = 9$, the aforementioned Nusselt number ratio was found to be about 1·73. From the present results, with $\Omega = 1{\cdot}35$ from equation (7), the ratio of the *local* mixed convection to forced convection Nusselt numbers is about 1·1 at the stagnation point and 1·3 at $\phi = 70°$. This comparison of analysis and experiment suggests that mixed convection effects are much larger on the aft portion of the cylinder than on the fore portion, with a shift in the separation point being highly likely. It might be noted that the experiments were performed with cylinders having only moderate length–diameter ratios and at fairly low Reynolds numbers (100 to 3000), and these factors might have affected the results.

REFERENCES

1. R. M. Fand and K. K. Keswani, Combined natural and forced convection heat transfer from horizontal cylinders to water, *Int. J. Heat Mass Transfer* **16**, 1175–1191 (1973).
2. P. H. Oosthuizen and S. Madan, The effect of flow direction on combined convective heat transfer from cylinders to air, *J. Heat Transfer* **C93**, 240–242 (1971).
3. B. Gebhart and L. Pera, Mixed convection from long horizontal cylinders, *J. Fluid Mech.* **45**, 49–64 (1970).
4. P. H. Oosthuizen and S. Madan, Combined convective heat transfer from horizontal cylinders in air, *J. Heat Transfer* **C92**, 194–196 (1970).
5. A. P. Hatton, D. D. James and H. W. Swire, Combined forced and natural convection with low-speed air flow over horizontal cylinders, *J. Fluid Mech.* **42**, 17–31 (1970).
6. G. K. Sharma and S. P. Sukhatme, Combined free and forced convection heat transfer from a heated tube to a transverse air stream, *J. Heat Transfer* **C91**, 457–459 (1969).
7. B. G. Van Der Hegge Zijnen, Modified correlation formulae for the heat transfers by natural and by forced convection from horizontal cylinders, *Appl. Scient. Res.* **A6**, 129–140 (1956).
8. A. A. Acrivos, On the combined effect of forced and free convection heat transfer in laminar boundary layer flow, *Chem. Engng Sci.* **21**, 343–352 (1966).
9. H. H. Sogin and Y. S. Subramanian, Local mass transfer from circular cylinders in cross flow, *J. Heat Transfer* **C83**, 483–493 (1961).
10. N. Frössling, Calculation by series expansion of the heat transfer in laminar, constant-property boundary layers at nonisothermal surfaces, *Ark. Fys.* **14**, 143–151 (1958).
11. H. Schlichting, *Boundary Layer Theory*, 6th edn, pp. 154–162. McGraw-Hill, New York (1968).
12. T. Chiang and J. Kaye, On laminar free convection from a horizontal cylinder, Proc. Fourth U.S. Nat. Cong. Appl. Mech., 1213–1219 (1962).
13. J. C. Y. Koh and J. F. Price, Laminar free convection from a nonisothermal cylinder, *J. Heat Transfer* **C87**, 237–242 (1965).

Int. J. Heat Mass Transfer. Vol. 19, pp. 232–233. Pergamon Press 1976. Printed in Great Britain

A NOTE ON HEAT-TRANSFER MECHANISM AS APPLIED TO FLOWING GRANULAR MEDIA

J BROUGHTON† and J. KUBIE‡

(*Received* 9 *June* 1975)

NOMENCLATURE

- d, particle diameter [m];
- Fo_m, $\alpha\tau/d^2$ average Fourier number;
- $\bar{h}$, average film heat-transfer coefficient [W/m² K];
- k, effective thermal conductivity of granular medium [W/mK];
- k_g, gas thermal conductivity [W/mK];
- K, surface conductance [W/m² K];
- L, length of plate [m];
- Nu_c, Kd/k_g, contact Nusselt number;
- $\overline{Nu_d^*}$, $\bar{h}d/k_g$, average Nusselt number;
- $\overline{Nu_L}$, $\bar{h}L/k$, average Nusselt number;
- Nu_m, $\bar{h}d/k$, average Nusselt number;
- Pe_L, UL/α, Peclet number;
- Pe_L^*, $Pe_L(k/k_g)^2(d/L)^2$, Peclet number;
- U, velocity of moving granular medium [m/s].

Greek symbols

- α, effective thermal diffusivity of granular medium [m²/s];
- γ, experimental constant;
- τ, L/U, mean packet residence time [s];
- χ, experimental constant.

INTRODUCTION

OVER the last twenty years there has been a continued interest in the mechanism of heat transfer between granular media and surfaces, as in dense-phase conveying, or in fluidized beds. Several mechanisms of heat transfer have been considered, however, two main approaches can be discerned; the packed-bed approach as used by Mickley and Fairbanks [1] and Baskakov [2] for example; and the single particle approach as used by Botterill and Williams [3] and Ziegler and Agrawal [4]. The recent paper by Sullivan and Sabersky [5] proposed two models describing heat transfer in flowing granular media; the former similar to that of Gabor [6]; the latter identical to that of Baskakov [7] (a modified Mickley–Fairbanks approach). As the interesting paper by Sullivan and Sabersky discounted the wide literature of the fluidized bed field, it is worthwhile and instructive to consider and analyze their data and conclusions in the light of fluidized bed heat-transfer knowledge.

†Unilever Research Ltd., Sharnbrook, Bedford, England.
‡Central Electricity Research Laboratories, Leatherhead, Surrey, England.

THEORETICAL CONSIDERATIONS

One of the traditional approaches to heat transfer in moving granular media has been to solve the transient heat-transfer equations during the time of contact, or the mean residence time of the medium on the surface, τ, which can be readily derived from the variables used by Sullivan and Sabersky by transforming

$$\tau = L/U.$$

The groups most commonly used in transient conduction studies can then readily be related to those used by Sullivan and Sabersky, as shown in Table 1.

Table 1. Transformation of variables

Usual variable		Sullivan and Sabersky [5] form
Fo_m	$\dfrac{\alpha\tau}{d^2}$	$(Pe_L)^{-1}\left(\dfrac{L}{d}\right)^2$
		$(Pe_L^*)^{-1}\left(\dfrac{k}{k_g}\right)^2$
Nu_m	$\dfrac{\bar{h}d}{k}$	$\overline{Nu_L}\dfrac{d}{L}$
		$\overline{Nu_d^*}\dfrac{k_g}{k}$
Nu_c	$\dfrac{dK}{k_g}$	$1/\chi$